Extending the limits of stabilizability of systems with feedback delay via fractional-order PD controllers

Tamas Balogh* Tamas Insperger**

** Department of Applied Mechanics, Budapest University of Technology and Economics, Budapest, Hungary (e-mail: baloghtamas2727@gmail.com).*
*** Department of Applied Mechanics, Budapest University of Technology and Economics and MTA-BME Lendület Human Balancing Research Group, Budapest, Hungary (e-mail: insperger@mm.bme.hu).*

Abstract: In the last few decades the advantages of fractional-order control was demonstrated with several examples in comparison with integer-order control. In this paper, stabilizability of a second-order unstable system subject to a delayed PD^{μ} and $PD^{\mu}D^{\rho}$ controller is investigated in terms of the critical delay. Stabilizability diagrams are determined as a function of the order of the fractional derivatives. It is shown that the critical delay for the PD^{μ} controller is larger by 12% than that of the PD^1 (or simply proportional-derivative, PD) controller and the critical delay for the $PD^{\mu}D^{\rho}$ controller is larger by 3.8% than the critical delay of the PD^1D^2 (or simply proportional-derivative-acceleration, PDA) controller.

Keywords: fractional-order control, stability, stabilizability, time delay.

1. INTRODUCTION

Stabilization of unstable equilibria in the presence of feedback delay is a challenging task. It is known that the extent of stabilizability of an inverted pendulum via delayed proportional-derivative (PD) feedback is limited: if the delay is larger than a critical value, then the system cannot be stabilized (Schurer, 1948; Stepan, 2009). It is also known that feeding back the acceleration, i.e., employing a proportional-derivative-acceleration (PDA) feedback, increases the critical delay by a factor of $\sqrt{2}$ compared to the PD feedback (Sieber and Krauskopf, 2005; Insperger et al., 2013). The goal of this paper is to investigate whether the critical delay can further be increased by introducing fractional-order derivates in the feedback loop. The correpsonding control law can be considered as a kind of transition between PD and PDA controllers (Dabiri et. al, 2018, Wang and Zheng, 2009). In this paper, a fractional-order $PD^{\mu}D^{\rho}$ controller is investigated, which, in case of $\mu = \rho = 1$ gives the PD feedback and for $\mu = 1$, $\rho = 2$ gives the PDA feedback as special limit cases.

1.1 Fractional derivative

There exist many different definitions of the fractional-order derivative in the literature. One of the most frequently used definitions is the Caputo fractional derivative, which is based on the generalization of the order of the *n*-fold integral to positive real numbers. The Caputo fractional derivative of order α with lower limit t_0 is defined as

$$ {}_{t_0}^{t}D_{*}^{\alpha} f(t) := \begin{cases} \dfrac{1}{\Gamma(m-\alpha)} \displaystyle\int_{t_0}^{t} (t-\tau)^{m-\alpha-1} f^{(m)}(\tau)\,\mathrm{d}\tau\,, & m-1<\alpha<m\,, \\ \dfrac{\mathrm{d}^{m}}{\mathrm{d}t^{m}} f(t)\,, & \alpha = m\,, \end{cases} \quad (1) $$

where $m \in \mathbb{N}$, and $\Gamma(x)$ is the gamma function (Podlubny, 1999). If $t_0 = 0$, then the Laplace transform of the Caputo fractional derivative of function *f* reads

$$ \mathcal{L}\left({}_{0}^{t}D_{*}^{\alpha} f(t)\right) = s^{\alpha}F(s) - \sum_{k=0}^{m-1} s^{\alpha-k-1} f^{(k)}(0)\,. \quad (2) $$

1.2 Stability of fractional differential equations

Stability of linear fractional differential equations with constant coefficients can be analysed by means of the corresponding characteristic equation, which, in general, has the form

$$ s^{\alpha_n} + \sum_{i=1}^{n-1} A_i\, s^{\alpha_i} + A_0 = 0\,. \quad (3) $$

A system associated with characteristic equation (3) is BIBO (Bounded Input Bounded Output) stable if and only if the roots of the characteristic equation have negative real part on the first Riemann sheet (Matignon, 1996; Monje et al., 2010).

Let us assume that the exponents α_i are rational numbers in (3), and let M be the least common multiple of the denominators of the exponents α_i. Then, using the substitution $\lambda = s^{\frac{1}{M}}$, the characteristic function on the left-hand side of (3) can be transformed into a polynomial of λ. The system is BIBO stable if and only if for the roots λ_i of this polynomial satisfy $|\arg(\lambda_i)| > \frac{1}{M}\frac{\pi}{2}$ (Matignon, 1996; Monje et al., 2010). The stable domain in the *s*-plane and in the λ-plane is shown in Figure 1. For retarded fractional-order time-delay systems, the stability condition is the same: the system is BIBO stable if and only if the roots of the characteristic equation have negative real part on the first Riemann sheet (Bonnet and Partington, 2002).

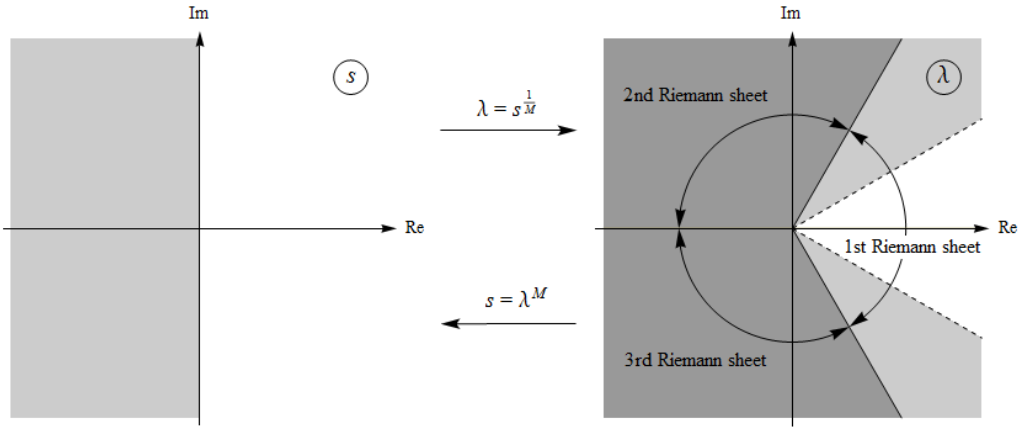

Fig. 1. The stable domain in the s-plane and in the λ-plane with $M = 3$.

2. PROBLEM FORMULATION

In Section 3, we study the BIBO stability of the second-order unstable plant subject to delayed PD$^{\mu}$ controller in the form

$$\frac{\mathrm{d}^2 y(t)}{\mathrm{d}t^2} - a_0\, y(t) = k_\mathrm{p}\, e(t-\tau) + k_\mathrm{d}\, {}_0^t D_*^{\mu} e(t-\tau)\,, \qquad (4)$$

where $a_0 > 0$ is the system parameter, k_p and k_d are the proportional and the derivative gains, $0 < \mu < 2$ is the order of the fractional derivative and τ is the feedback delay. Let $u_\mathrm{r}(t)$ be the reference input. Then the error signal $e(t)$ can be written as $e(t) = u_\mathrm{r}(t) - y(t)$. After introducing the dimensionless time $\vartheta = t/\tau$, (4) can be written in the form

$$\frac{\mathrm{d}^2 y(\vartheta)}{\mathrm{d}\vartheta^2} - a\, y(\vartheta) = p\, e(\vartheta - 1) + d\, {}_0^{\vartheta} D_*^{\mu} e(\vartheta - 1), \qquad (5)$$

where $a = a_0\tau^2,\ p = k_p\tau^2,\ d = k_d\tau^{2-\mu}$. The corresponding characteristic function is

$$D(s) = s^2 - a + p\, e^{-s} + d\, s^{\mu} e^{-s}\,. \qquad (6)$$

In Section 4, we investigate a more general case with PD$^{\mu}$D$^{\rho}$ feedback given by the differential equation

$$\frac{\mathrm{d}^2 y(t)}{\mathrm{d}t^2} - a_0\, y(t) = k_\mathrm{p}\, e(t-\tau) + k_{\mathrm{d},1}\, {}_0^t D_*^{\mu} e(t-\tau) + k_{\mathrm{d},2}\, {}_0^t D_*^{\rho} e(t-\tau)\,, \qquad (7)$$

where $0 < \mu, \rho < 2$. The characteristic function of (7) is

$$D(s) = s^2 - a_0 + k_\mathrm{p}\, e^{-s\tau} + k_{\mathrm{d},1}\, s^{\mu} e^{-s\tau} + k_{\mathrm{d},2}\, s^{\rho} e^{-s\tau}. \qquad (8)$$

Special cases of (7) are as follows.

The case $\mu = 1$ and $k_{\mathrm{d},2} = 0$ gives a PD (or PD^1) feedback of integer order. In this case, the critical delay can be given as (Schurer, 1948; Stepan, 2009)

$$\tau_{\mathrm{crit,PD}} = \sqrt{2/a_0}. \qquad (9)$$

This means that there is no pair $(k_\mathrm{p}, k_{\mathrm{d},1})$, which can stabilize the system if the feedback delay is larger than $\tau_{\mathrm{crit,PD}}$.

The case $\mu = 1$ and $\rho = 2$ gives a PDA (or PD^{1}D^2) controller. The corresponding critical delay is (Sieber and Krauskopf, 2005)

$$\tau_{\mathrm{crit,PDA}} = \sqrt{4/a_0} = \sqrt{2}\,\tau_{\mathrm{crit,PD}} \qquad (10)$$

that is larger than $\tau_{\mathrm{crit,PD}}$ by a factor of $\sqrt{2} = 1.41$. This means that there is no stabilizing triple $(k_\mathrm{p}, k_{\mathrm{d},1}, k_{\mathrm{d},2})$ if $\tau > \tau_{\mathrm{crit,PDA}}$.

3. STABILIZABILITY OF THE SYSTEM WITH PD$^{\mu}$ CONTROLLER

In this section we determine the stability map of (5) using the D-subdivision method (Hamamci, 2007) and we construct the corresponding stabilizability diagram as function of the derivative order μ.

3.1 Stability map

According to the D-subdivision method, the stability map can be divided into domains, where the number of unstable roots is constant. These domains are bounded by three types of boundaries: the RRB (Real Root Boundary), the IRB (Infinite Root Boundary), and the CRB (Complex Root Boundary), which can be determined using the equations $D(0) = 0$, $\lim_{|s|\to\infty} D(s) = 0$, and $D(\pm \mathrm{i}\, x) = 0, x \in \mathbb{R}^+$, respectively (Hamamci, 2007). The equation of the RRB D-curve is

$$p = a\,. \qquad (11)$$

The parametric equation of the CRB D-curve is

$$p = \frac{(x^2 + a)\sin\left(\mu\frac{\pi}{2} - x\right)}{\sin\left(\mu\frac{\pi}{2}\right)}, \qquad (12)$$

$$d = \frac{(x^2 + a)\sin(x)}{x^{\mu}\sin\left(\mu\frac{\pi}{2}\right)}, \qquad (13)$$

where $x > 0$ is the running parameter. For system (5), there is no IRB D-curve. The number of unstable roots in the domains can be determined using a numerical method

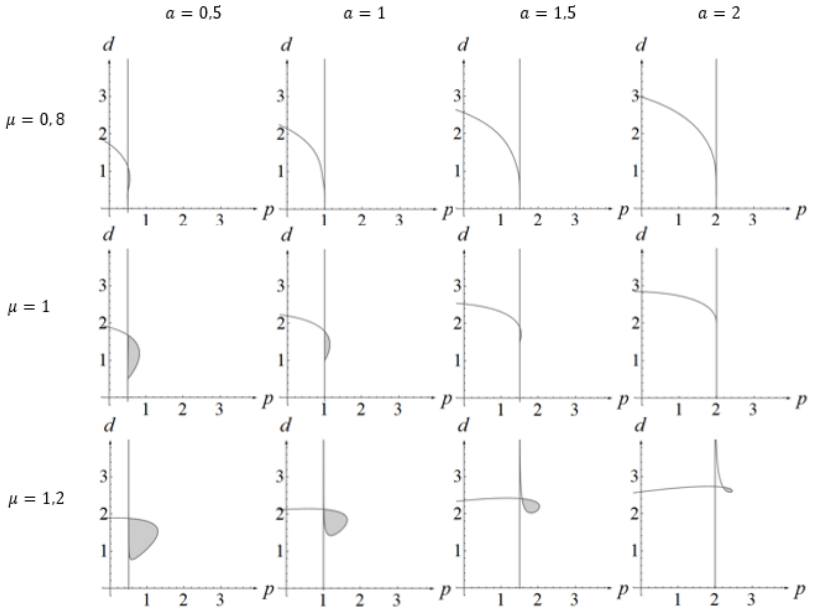

Fig. 2. Stability charts for (5) for different values of a and μ.

developed by Merrikh-Bayat (2013). The stability charts for (5) for different values of a and μ are shown in Figure 2. The BIBO stable regions are indicated by grey shading.

3.2 Stabilizability diagram

Figure 2 shows that for a fixed μ the stable domain shrinks as a is increased, and at $a = a_{\max}$ it completely disappears. The value $a_{\max}$ can be called the stabilizability limit. The stable domain is bounded by only the initial part of the CRB D-curve, therefore it is sufficient to consider the CRB D-curve with $0 < x < \mu\frac{\pi}{2}$. The stabilizability limit $a_{\max}(\mu)$ can be determined differently for $0 < \mu < 1$ and for $1 < \mu < 2$ because the conditions for the loss of stabilizability are different in these cases.

If $0 < \mu < 1$, then for $a = a_{\max}$ the RRB line is tangent to the CRB D-curve. At the point of tangency, equations (11), (12), and (13) hold, and the function $p(x)$ has a local maximum, therefore the derivative of $p(x)$ with respect to x is zero. Using these conditions, we can calculate the parametric equation of the curve $a_{\max}(\mu)$. This parametric equation can be given in two parts as

$$\mu_{1,2} = \frac{2}{\pi}\operatorname{arctg}\left(\frac{-4\sin(x)\cos(x)+2\sin(x)+x\cos(x)\pm\sqrt{\Delta(x)}}{2(-2\cos^2(x)+2\cos(x)-x\sin(x))}\right), \quad (14)$$

$$a_{\max 1,2} = \frac{x^2\sin\left(\mu_{1,2}\frac{\pi}{2}-x\right)}{\sin\left(\mu_{1,2}\frac{\pi}{2}\right)-\sin\left(\mu_{1,2}\frac{\pi}{2}-x\right)}, \quad (15)$$

where $\Delta(x) = 4\sin^2(x) + x^2\cos^2(x) + 4x\sin(x)\cos(x) - 8x\sin(x)$. The domain of both parts is $(0, x_{\max}]$ and the two pieces have the same value at $x = x_{\max}$, so $\Delta(x_{\max}) = 0$. Therefore $x_{\max}$ is a root of the equation $\Delta(x) = 0$, and it satisfies the condition $0 < x_{\max} < \mu\frac{\pi}{2} < \frac{\pi}{2}$. The numerically calculated value is $x_{\max} = 0.543358$.

If $1 < \mu < 2$, then the stable domain is bounded by the loop of the CRB D-curve (see Figure 2). The value of a where the loop disappears can be determined numerically by stepwise increasing a from $a = 0$ and checking the existence of the loop. Therefore the values of the function $a_{\max}(\mu)$ can be determined for $1 < \mu < 2$.

The overall stabilizability limit for $0 < \mu < 2$ is shown in Figure 3. For the PD controller the stabilizability limit is $a_{\max}(\mu = 1) = 2$ (Insperger and Stepan, 2011). It can be seen that the stabilizability limit can be extended using a PD$^\mu$ controller. The maximum value of the function $a_{\max}(\mu)$ is $a^*_{\max} = a_{\max}(\mu^*) = 2.5066$, where $\mu^* = 1.106$ is the order of the fractional derivative.

Rephrasing the results in terms of the critical delay, we can conclude that for a fixed system parameter the critical delay for the PD$^\mu$ controller is

$$\tau_{\text{crit,PD}^\mu} = \sqrt{2.5066/a_0} \approx 1.12\,\tau_{\text{crit,PD}}. \quad (16)$$

Thus, the critical delay of a PD feedback can be increased by 12% if fractional order derivatives are used.

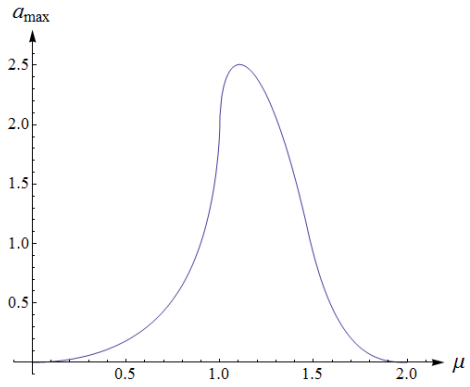

Fig. 3. The function $a_{\max}(\mu)$ corresponding to the stabilizability limit for $0 < \mu < 2$.

4. STABILIZABILITY OF THE SYSTEM WITH PD$^{\mu}$D$^{\rho}$ CONTROLLER

While (4) was transformed into the dimensionless form (5) in case of the PD$^{\mu}$ controller, we will analyse (7) without any time transformation. We assume that parameter a_0 is fixed in (7), and we determine the maximal time delay $\hat{\tau}_{\max}$ for which the system is stable using the numerical method described in Fioravanti et al. (2011) and Pakzad and Pakzad (2012). Without loss of generality, we assume that $a_0 = 1$ in (7). Then we can calculate the dimensionless stabilizability limit with the equation $\hat{a}_{\max} = a_0\, \hat{\tau}_{\max}^2 = \hat{\tau}_{\max}^2$.

The stabilizability limit $\hat{a}_{\max}$ determined for fixed parameters is a function of the controller coefficients (k_{p}, $k_{\mathrm{d},1}$, $k_{\mathrm{d},2}$) and the derivative orders (μ, ρ). We can determine the stabilizability limit $a_{\max}$ as a function of the derivative orders by maximizing $\hat{a}_{\max}$ with respect to k_{p}, $k_{\mathrm{d},1}$, and $k_{\mathrm{d},2}$.

4.1 Purely imaginary roots of the characteristic equation

Assume that the derivative orders are rational numbers, i.e. they can be written as $\mu = \frac{m}{M}$ and $\rho = \frac{r}{M}$, where m, r, and M are positive integers. Then the characteristic function can be written in the form

$$D(s;\tau) = p_0(s^{\gamma}) + p_1(s^{\gamma})\, e^{-s\tau}\,, \tag{17}$$

where $\gamma = \frac{1}{M}$. The polynomials $p_0(x)$ and $p_1(x)$ read

$$p_0(x) = x^{2M} - a_0 = x^{2M} - 1\,, \tag{18}$$

$$p_1(x) = k_{\mathrm{p}} + k_{\mathrm{d},1}\, x^m + k_{\mathrm{d},2}\, x^r\,. \tag{19}$$

The goal of the numerical method is to determine the τ values for which the characteristic equation has a purely imaginary root. For this purpose, we first have to find the roots which have the form $s = \mathrm{i}\omega$, where $\omega > 0$. The imaginary part of these roots coincide with the positive real roots of the equation (Pakzad and Pakzad, 2012)

$$p_0((\mathrm{i}\omega)^{\gamma})\, p_0((-\mathrm{i}\omega)^{\gamma}) - p_1((\mathrm{i}\omega)^{\gamma})\, p_1((-\mathrm{i}\omega)^{\gamma}) = 0\,. \tag{20}$$

Using the substitution $u = \omega^{\gamma} = \omega^{\frac{1}{M}}$, (20) can be written in the form

$$p_0(\mathrm{i}^{\gamma}u)\, p_0((-\mathrm{i})^{\gamma}u) - p_1(\mathrm{i}^{\gamma}u)\, p_1((-\mathrm{i})^{\gamma}u) = 0\,. \tag{21}$$

After some algebraic manipulation, we obtain the following polynomial equation of degree $4M$:

$$\begin{aligned} u^{4M} + 2u^{2M} - k_{\mathrm{d},1}^2 u^{2m} - 2\, k_{\mathrm{d},1}\, k_{\mathrm{d},2} \cos\left(\tfrac{m-r}{M}\,\tfrac{\pi}{2}\right) u^{m+r} \\ -k_{\mathrm{d},2}^2 u^{2r} - 2\, k_{\mathrm{p}}\, k_{\mathrm{d},1} \cos\left(\tfrac{m}{M}\,\tfrac{\pi}{2}\right) u^{m} \\ -2\, k_{\mathrm{p}}\, k_{\mathrm{d},2} \cos\left(\tfrac{r}{M}\,\tfrac{\pi}{2}\right) u^{r} + \left(1 - k_{\mathrm{p}}^2\right) = 0\,. \end{aligned} \tag{22}$$

After calculating the positive real roots of this polynomial, the positive real roots of (20) can be calculated using the equation $\omega = u^M$. For the so obtained ω values there is a time delay τ, for which $s = \mathrm{i}\omega$ is a root of the characteristic function (17).

4.2 Time delays and root tendency

For the purely imaginary roots $\mathrm{i}\omega_i$, the corresponding time delays can be determined using (17) as

$$\tau_{k,i} = -\tfrac{1}{\omega_i}\arg\left(-\tfrac{p_0((\mathrm{i}\omega_i)^{\gamma})}{p_1((\mathrm{i}\omega_i)^{\gamma})}\right) + \tfrac{1}{\omega_i} k2\pi\,,\ k \in \mathbb{Z}\,. \tag{23}$$

This equation for the polynomials (18) and (19) has the form

$$\begin{aligned} \tau_{k,i} = \frac{1}{\omega_i}\arg\left(k_{\mathrm{p}} + k_{\mathrm{d},1}\, \omega_i^{\frac{m}{M}} e^{\mathrm{i}\frac{m}{M}\frac{\pi}{2}} + k_{\mathrm{d},2}\, \omega_i^{\frac{r}{M}} e^{\mathrm{i}\frac{r}{M}\frac{\pi}{2}}\right) \\ + \frac{1}{\omega_i} k2\pi\,, \qquad k \in \mathbb{Z}\,. \end{aligned} \tag{24}$$

Using the notation $\Delta\tau_i = \frac{2\pi}{\omega_i}$, (24) can be written as

$$\tau_{k,i} = \tau_{0,i} + k\, \Delta\tau_i\,, \qquad k \in \mathbb{Z}\,. \tag{25}$$

This arithmetic sequence gives the infinitely many time delays $\tau_{k,i}$, for which $\mathrm{i}\omega_i$ is a root of the characteristic equation.

The root tendency RT_i corresponding to $\mathrm{i}\omega_i$ can be calculated as follows:

$$RT_i = \operatorname{sgn}\left(\operatorname{Re}\left(-\frac{\frac{\partial D(\mathrm{i}\omega_i;\tau_{k,i})}{\partial\tau}}{\frac{\partial D(\mathrm{i}\omega_i;\tau_{k,i})}{\partial s}}\right)\right). \tag{26}$$

Note that the root tendency RT_i is independent of k (Fioravanti et al., 2011; Pakzad and Pakzad, 2012).

4.3 Number of unstable roots for $\tau = 0$

If $\tau = 0$, then the characteristic function reads

$$D_0(s) = s^2 - 1 + k_{\mathrm{p}} + k_{\mathrm{d},1}\, s^{\frac{m}{M}} + k_{\mathrm{d},2}\, s^{\frac{r}{M}}\,. \tag{27}$$

Using the substitution $\lambda = s^{\gamma} = s^{\frac{1}{M}}$, (27) can be written as

$$D_0(\lambda) = \lambda^{2M} + k_{\mathrm{d},1}\, \lambda^m + k_{\mathrm{d},2}\, \lambda^r + k_{\mathrm{p}} - 1\,. \tag{28}$$

Let s_j be the roots of the characteristic function (27), and let λ_j be the roots of (28). Then, the number of unstable roots (i.e. the number of roots s_j with nonnegative real part on the first Riemann-sheet) is equal to the number of roots λ_j satisfying $\left|\arg(\lambda_j)\right| \le \frac{1}{M}\frac{\pi}{2}$. Therefore, after calculating the roots of (28), the number of unstable roots for $\tau = 0$ can be determined.

4.4 Stabilizability limit for fixed parameters

After determining the $\tau_{k,i}$ sequences and the root tendencies, the positive number line of the time delay values can be divided into subintervals by the time delays $\tau_{k,i}$. The number

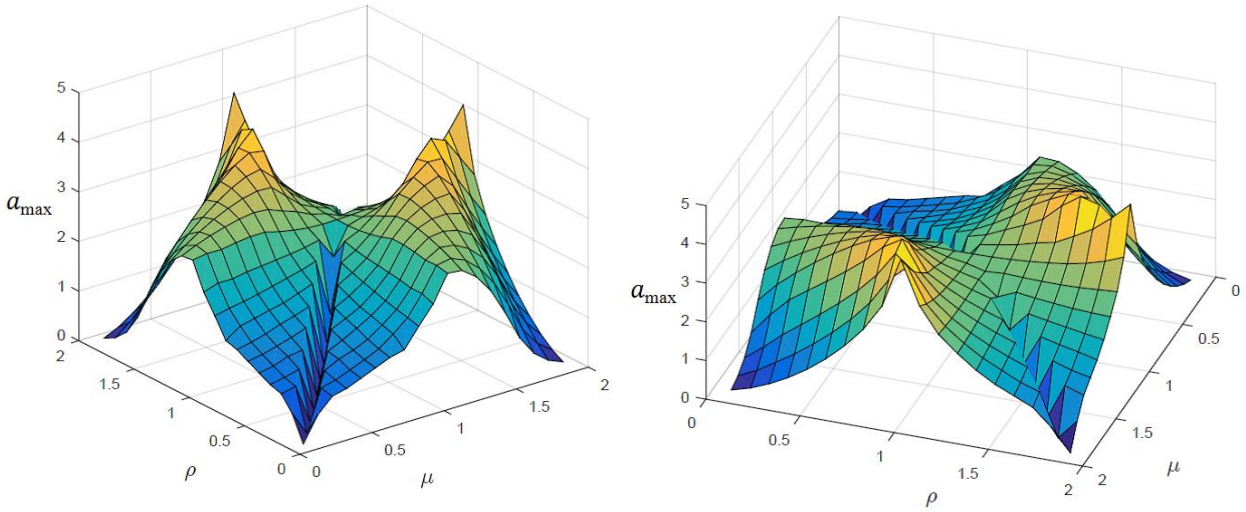

Fig. 4. Views of the function $a_{\max}(\mu, \rho)$ corresponding to the stabilizability limit for $0 < \mu, \rho < 2$.

of unstable roots is constant in these subintervals, and it changes by $2RT_i$ at $\tau = \tau_{k,i}$. System (7) is delay equation of retarded type, so the number of unstable roots in the first subinterval is equal to the number of unstable roots for $\tau = 0$ (Fioravanti et al., 2011).

In order to determine the stabilizability limit $\hat{a}_{\max}$, we have to assume that $\hat{\tau}_{\max}$ is smaller than some time delay $\tilde{\tau}$. Then we can determine those elements of the sequences $\tau_{k,i}$ which fall in the interval $[0, \tilde{\tau}]$. After, this interval can be divided into subintervals, and the number of unstable roots can be determined. If the number of unstable roots in a subinterval is zero, then the subinterval is stable; otherwise it is unstable. The upper bound of the last stable subinterval is equal to $\hat{\tau}_{\max}$. Then the stabilizability limit can be calculated as $\hat{a}_{\max} = \hat{\tau}_{\max}^2$.

For the PDA controller the stabilizability limit is $a_{\max}(\mu = 1, \rho = 2) = 4$ (Sieber and Krauskopf, 2005).

4.5 Stabilizability limit as a function of the derivative orders

To determine the stabilizability limit $a_{\max}$, we have to maximize the function $\hat{a}_{\max}(k_{\mathrm{p}}, k_{\mathrm{d},1}, k_{\mathrm{d},2}, \mu, \rho)$ with respect to k_{p}, $k_{\mathrm{d},1}$, and $k_{\mathrm{d},2}$. This function is a black-box function, i.e. its analytic form is not known. Direct search is a possible way of optimizing black-box functions, therefore we used a specific direct search technique, the pattern search method for the optimization (Lewis et al., 2000).

If the denominator M increases in the derivative orders $\mu = \frac{m}{M}$ and $\rho = \frac{r}{M}$, then the degrees of the polynomial equations (22) and (28) also increase. Therefore we set $M = 10$ to reduce the computational cost. The parameters m and r take the values $m = 1, 2, \ldots, 2M - 1$ and $r = 1, 2, \ldots, 2M - 1$.

Views of the stabilizability limit as a function of the derivative orders for $0 < \mu, \rho < 2$ are shown in Figure 4. The graph of the function is symmetric about the plane $\mu = \rho$. The function values along the line $\mu = \rho$ in the plane (μ, ρ) correspond to the values of the stabilizability limit $a_{\max}(\mu)$ for the PD$^{\mu}$ controller. The maximum value of the function $a_{\max}(\mu, \rho)$ determined with $M = 10$ is $a_{\max} = 4.2308$ at $\mu = 1, \rho = 1.9$.

The maximum value of the function determined with $M = 100$ in the neighbourhood of the point $\mu = 1, \rho = 1.9$ is $a_{\max}^* = a_{\max}(\mu^*, \rho^*) = 4.3108$, where $\mu^* = 0.99$, $\rho^* = 1.85$ is the maximum point. Therefore the PD$^{\mu}$D$^{\rho}$ controller shows better stabilizability properties than the PD, the PD$^{\mu}$, and the PDA controllers.

Rephrasing the results for the PD$^{\mu}$D$^{\rho}$ controller in terms of the critical delay, we can conclude that for a fixed system parameter the critical delay for the PD$^{\mu}$ controller is

$$\tau_{\mathrm{crit,PD}^{\mu}\mathrm{D}^{\rho}} = \sqrt{4.3108/a_0}\, \tau_{\mathrm{crit,PDA}} \approx 1.038\, \tau_{\mathrm{crit,PDA}}\,. \qquad (29)$$

Thus, the critical delay of a PDA feedback can be increased by 3.8% if fractional order derivatives are used instead of integer orders.

5. CONCLUSIONS

Stabilizability of a second-order unstable plant subject to fractional-order delayed feedback was analysed in terms of the critical feedback delay. It was shown that the critical delay for the PD$^{\mu}$ controller with $\mu = 1.106$ is larger by 12% than that of the PD controller and the critical delay for the PD$^{\mu}$D$^{\rho}$ controller with $\mu = 0.99$ and $\rho = 1.85$ is larger by 3.8% than the critical delay of the PDA controller. Thus, introducing fractional order derivatives into the control law improves stabilizability properties for large feedback delays.

It should be mentioned that this analysis was performed only for the ideal case when all the parameters are perfectly known. Stability diagram for the PD$^{\mu}$D$^{\rho}$ controller was determined using a combination of the discrete approximation of the fractional-order derivative according the Grünwald-Letnikov definition (Podlubny, 1999) and the semidiscretization method (Insperger and Stepan, 2011). A

sample stability diagram is shown in Figure 5. The exact D-curve is shown by dashed line. The stable region was also determined numerically using a discretization step $\Delta t = \tau/r$ with delay resolution $r = 100$, and the $N = 100$ terms were used for the discrete approximation of the fractional derivative. It can be seen that the boundaries obtained numerically does not coincide with the D-curve. This demonstrates the sensitivity of the application of fractional order controllers. Issues related to the weak robustness of the Grünwald-Letnikov derivative can be handled by using predictor-corrector methods (Wang, 2017).

It should also be mentioned that stabilization in the presence of large feedback delays can also be realized using other techniques. Predictor feedback (Krstic, 2009), event-driven intermittent controller (Yoshikawa et al., 2016) or the time driven intermittent controllers, such as the act-and-wait concept (Insperger and Stepan, 2011) can be mentioned as examples. A simple but effective technique is the application of a detuned PD control, where the different feedback terms are associated with different delays. As shown by Sieber and Krauskopf (2005), the critical delay for the detuned PD controller is $\tau_{\text{crit,detuned-PD}} = 1.039\,\tau_{\text{crit,PDA}}$, which is slightly larger than the critical delay for the fractional-order PD$^{\mu}$D$^{\rho}$ feedback.

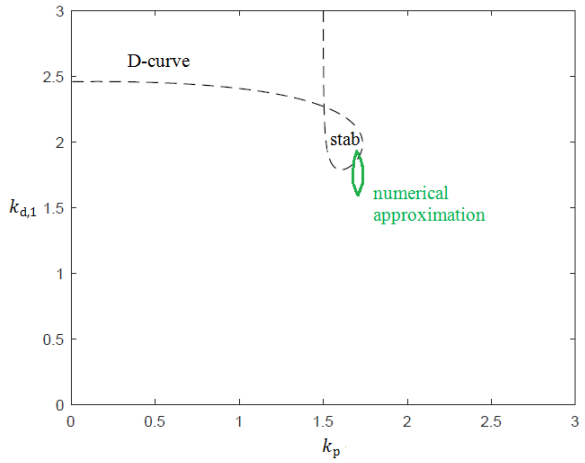

Fig. 5. Stability diagram for (7) with $a_0 = 1.5$, $\tau = 1$, $\mu = 1.1$, $k_{d,2} = 0$.

REFERENCES

Bonnet, C. and Partington, J.R. (2002). Analysis of fractional delay systems of retarded and neutral type. *Automatica*, 38(7), 1133–1138.

Dabiri, A., Butcher, E., Poursina, M. and Nazari, M. (2018). Optimal periodic-gain fractional delayed state feedback control for linear fractional periodic time-delayed systems. *IEEE Transactions on Automatic Control*. published online.

Fioravanti, A.R., Bonnet, C., Özbay, H., and Niculescu, S. (2011). Stability windows and unstable root-loci for linear fractional time-delay systems. *IFAC Proceedings Volumes*, 44(1), 12532–12537.

Hamamci, S.E. (2007). An algorithm for stabilization of fractional-order time delay systems using fractional-order PID controllers. *IEEE Transactions on Automatic Control*, 52(10), 1964–1969.

Insperger, T. (2006). Act-and-wait concept for time-continuous control systems with feedback delay. *IEEE Transactions on Control Systems Technology*, 14(5), 974-977.

Insperger, T., Milton, J., and Stépán, G. (2013). Acceleration feedback improves balancing against reflex delay. *Journal of the Royal Society Interface*, 10(79). 20120763.

Insperger, T. and Stépán, G. (2011). *Semi-Discretization for Time-Delay Systems – Stability and Engineering Applications*. Springer, New York.

Krstic, M. (2009). *Delay compensation for nonlinear, adaptive, and PDE systems*. Birkhäuser, Boston.

Lewis, R.M., Torczon, V., and Trosset, M.W. (2000). Direct search methods: then and now. *Journal of Computational and Applied Mathematics*, 124(1–2), 191–207.

Matignon, D. (1996). Stability results for fractional differential equations with applications to control processing. *Computational engineering in systems applications*, 2, 963–968.

Merrikh-Bayat, F. (2013). General formula for stability testing of linear systems with fractional-delay characteristic equation. *Open Physics*, 11(6), 855–862.

Monje, C.A., Chen, Y., Vinagre, B.M., Xue, D., and Feliu-Batlle, V. (2010). *Fractional-order systems and controls: fundamentals and applications*. Springer, London.

Pakzad, M.A. and Pakzad, S. (2012). Stability Map of Fractional Order Time-Delay Systems. *WSEAS Transactions on Systems*, 10(11), 541–550.

Podlubny, I. (1999). *Fractional differential equations*. Academic Press, San Diego.

Schurer, F. (1948). Zur theorie des balancierens. *Mathematische Nachrichten*, 1, 295–331.

Sieber, J. and Krauskopf, B. (2005). Extending the permissible control loop latency for the controlled inverted pendulum. *Dynamical Systems*, 20(2), 189–199.

Stepan, G. (2009). Delay effects in the human sensory system during balancing. *Philosophical Transactions of the Royal Society of London A: Mathematical, Physical and Engineering Sciences*, 367, 1195–1212.

Wang, Z.H. (2017). Personal communication.

Wang, Z.H. and Zheng, Y.G. (2009) The optimal form of the fractional-order difference feedbacks in enhancing the stability of a sdof vibration system. *Journal of Sound and Vibration*, 326(3–5), 476–488.

Yoshikawa, N., Suzuki, Y., Kiyono, K., and Nomura, T. (2016). Intermittent feedback-control strategy for stabilizing inverted pendulumon manually controlled cart as analogy to human stick balancing. *Frontiers in Computational Neuroscience*, 10, 39.